

Abstract

We introduce a Bayesian fusion scheme for the detection and the localization of targets using multiple sensors. This method could be useful in the field of sea mines detection where different kinds of sensors can be used. From an operational point of view, it is desirable to identify dangerous areas (a mine is present with significant probability), safe areas (high probability that there is no mine) and unknown areas (not enough information to conclude). We illustrate the method by the fusion of two independent fictive sensors and produce two dimensional risk maps for a single target. We extend the method for multiple targets and compare different ROC curves to evaluate its performances.

Bayesian map fusion

- Input: n sensors S_i , $i \in \{1, \dots, n\}$ provide $A_i(T_r) = \frac{p(Y_i|T_r)}{p(Y_i|\bar{T})}$
- Hypothesis 1: there is at most one target in the area V .
- Hypothesis 2: the sensors are independent

$$p(Y_1, \dots, Y_n|T_r) = \prod_{i=1}^n p(Y_i|T_r) \quad (1)$$

$$p(Y_1, \dots, Y_n|\bar{T}) = \prod_{i=1}^n p(Y_i|\bar{T}) \quad (2)$$

- Output: $p(T_r|Y_1, \dots, Y_n)$. This joint posterior probability distribution can be calculated as:

$$p(T_r|Y_1, \dots, Y_n) = \frac{(\prod_{i=1}^n A_i(T_r))A_0(T_r)}{1 + \int_V (\prod_{i=1}^n A_i(T_r))A_0(T_r)dr} \quad (3)$$

where $A_0(T_r)$ is the prior ratio $\frac{p(T_r)}{p(\bar{T})}$

Context

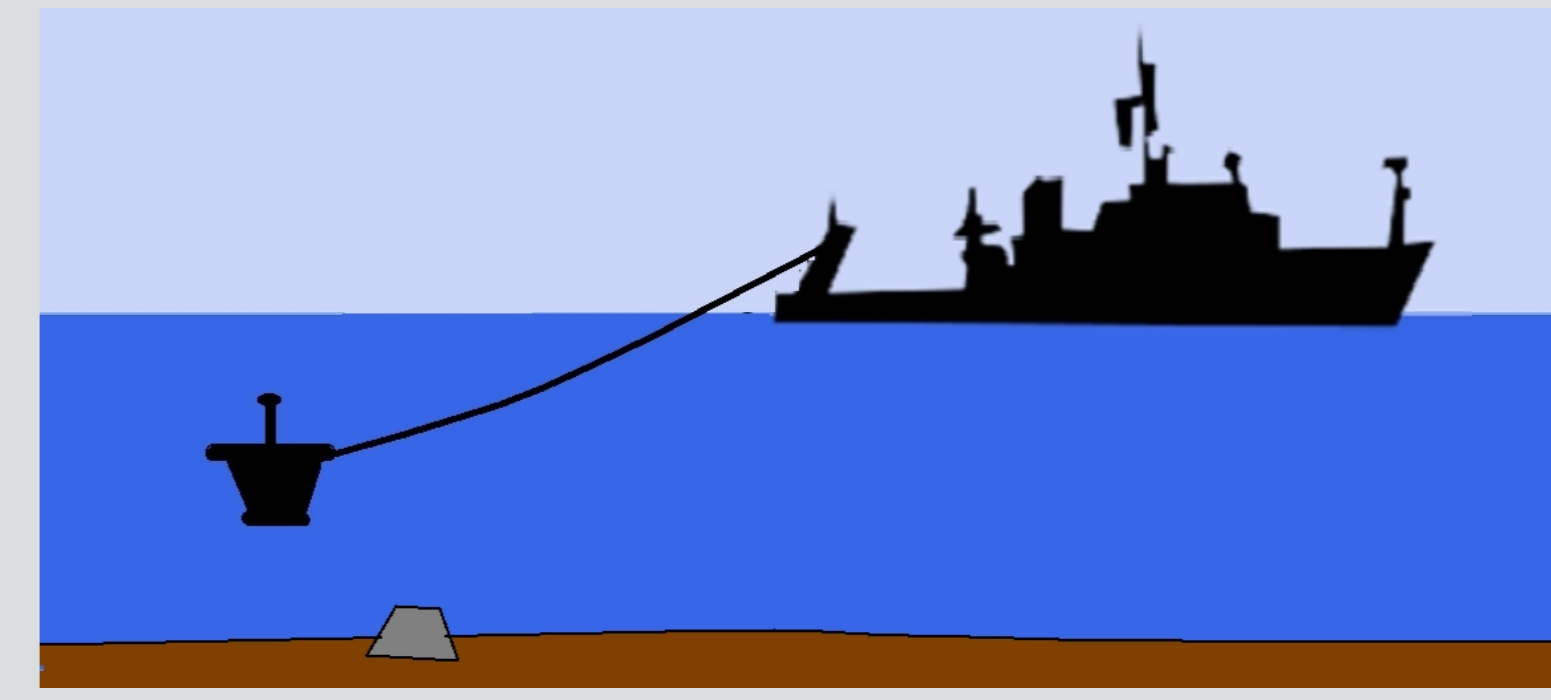


Figure 1: In the field of sea mines detection, several sensors can be used, such as sonars, magnetic gradiometers, electromagnetic sensors or electrochemical sensors. We propose a method to fuse the information from the different sensors to achieve better detection performances.

Simple sensor model

- Sensor S_1 : $R_1 = \{r_1^1, \dots, r_1^{n_1}\}$, $Y_1 = \{y(r_1^1), \dots, y(r_1^{n_1})\}$
- Sensor S_2 : $R_2 = \{r_2^1, \dots, r_2^{n_2}\}$, $Y_2 = \{y(r_2^1), \dots, y(r_2^{n_2})\}$
- Target parameters : $a_1 \sim p(a_1|T)$, $a_2 \sim p(a_2|T)$, $r_0 \sim \frac{p(T_r)}{p(\bar{T})}$
- Sensor model

$$y(r_i^j) = \begin{cases} \frac{a_i}{|r_i^j - r_0|^3} + \eta_i^j & \text{if there is a target} \\ \eta_i^j \sim N(0, \sigma_i) & \text{if there is no target} \end{cases} \quad (4)$$

- Likelihoods:

$$p(Y_i|\bar{T}) = \frac{1}{\sqrt{2\pi}\sigma_i} e^{-\frac{1}{2}\frac{Y_i Y_i^T}{\sigma_i^2}} \quad (5)$$

$$p(Y_i|T_r) = \int_{-\infty}^{+\infty} p(Y_i|a_i, T_r)p(a_i|T_r)da_i \\ = \int_{-\infty}^{+\infty} \frac{1}{\sqrt{2\pi}\sigma_i} e^{-\frac{1}{2}\frac{\sum_{j=1}^{n_i} (y_i^j - \frac{a_i}{|r_i^j - r_0|^3})^2}{\sigma_i^2}} p(a_i|T)da_i \quad (6)$$

Simulation results

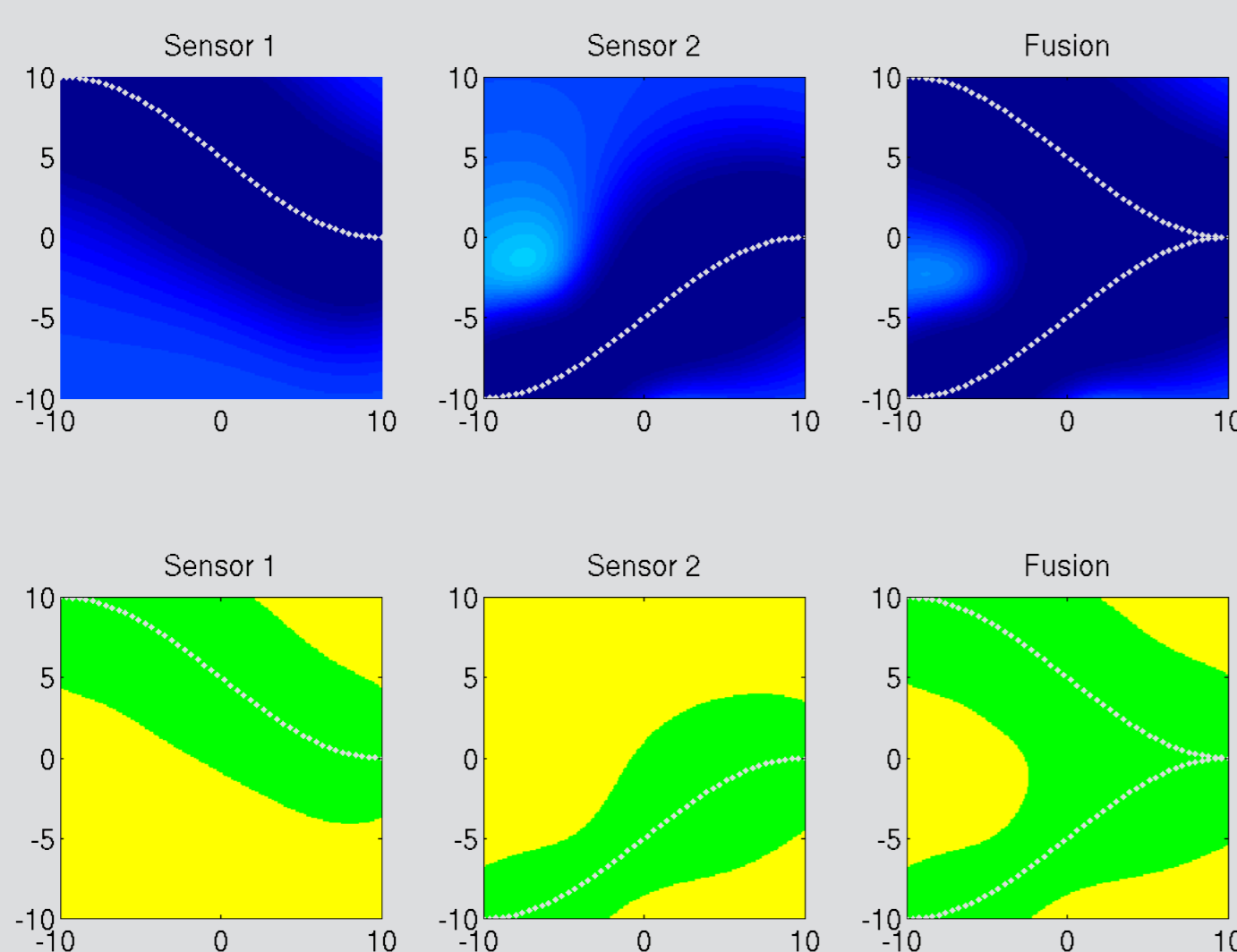


Figure 2: Posterior probability distributions (top) and associated risk maps (bottom) for sensor S_1 , S_2 and for the fusion in the absence of a target. The white curves correspond to the trajectories of the sensors. The green and the yellow colors correspond to safe and unknown areas.

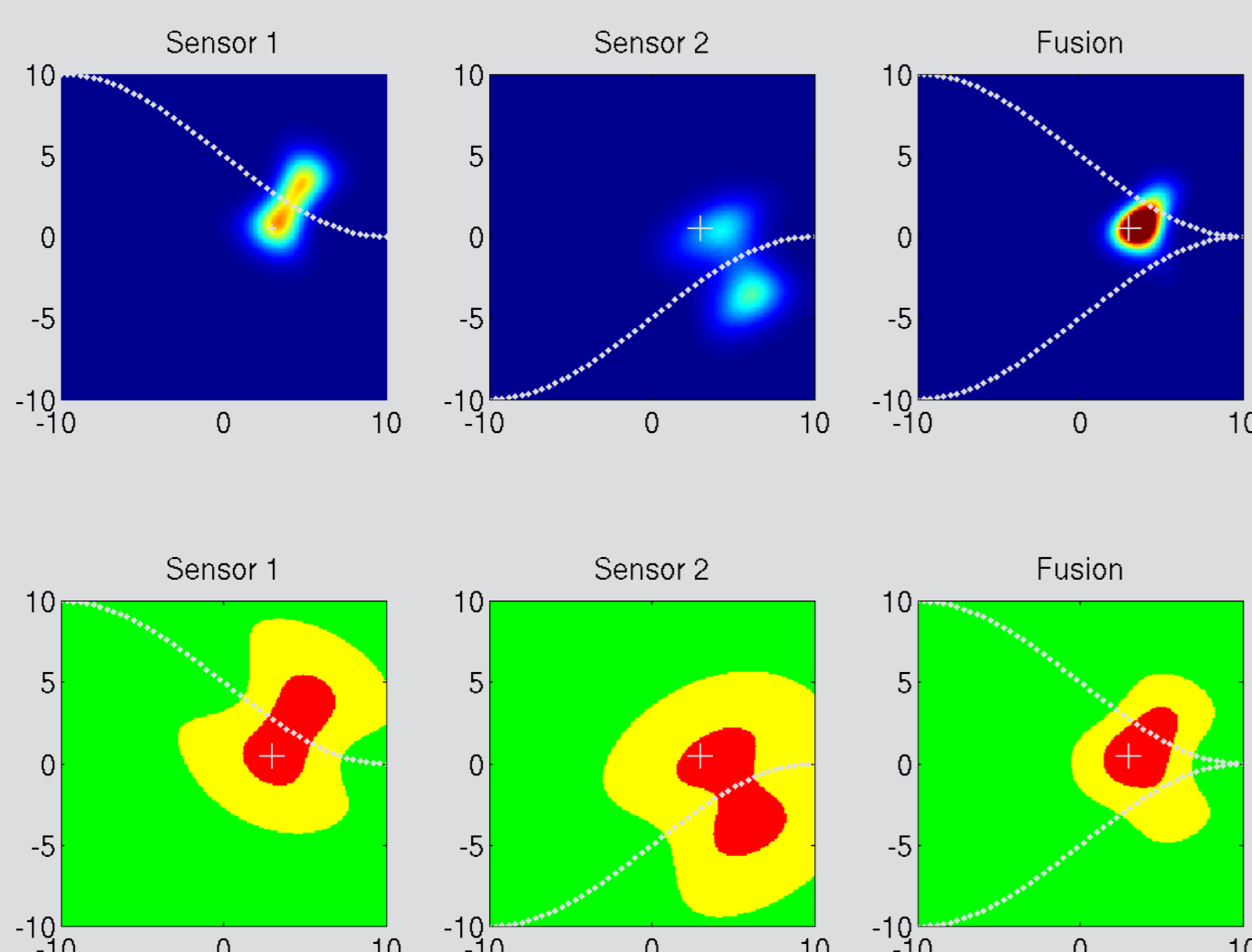


Figure 3: Posterior probability distributions (top) and associated risk maps (bottom) for sensor S_1 , S_2 and for the fusion in the presence of a single target. The cross is the actual position of the target. The red color corresponds to dangerous area.

Histogram test

- $N_e = 10^4$ simulations
- $P(T) = P(\bar{T}) = 1/2$
- $S_\alpha : P(r_0 \in S_\alpha | Y_1, Y_2) = \alpha$
- Test : $r_0 \in S_\alpha$: Bernoulli trial
- N tests : binomial distribution

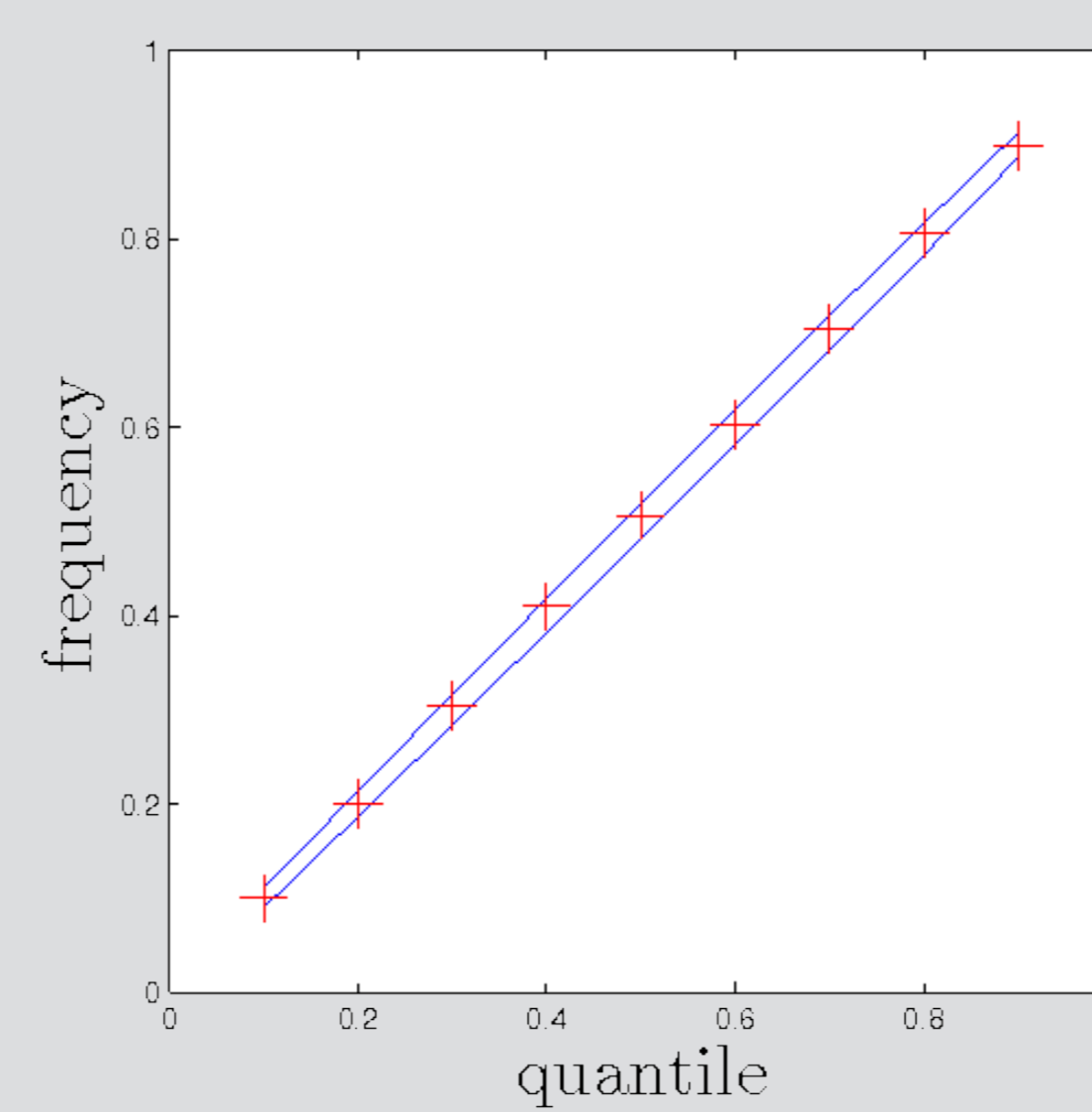


Figure 4: Frequency of the presence of the target in the region S_α as a function of the quantile α together with the Wilson confidence interval at 99% for the binomial distribution.

References

- [1] Eric Mersch, Yann Yvinec, Yves Dupont, Xavier Neyt, and Pascal Druyts. Underwater magnetic target localization and characterization using a three-axis gradiometer. In *OCEANS 2014-TAIPEI*, pages 1–6. IEEE, 2014.
- [2] P Druyts and M Acheroy. A modular multi-layer perceptron (mmlp) to identify objects composed of characteristic sub-parts. *Dagli, Akay, Fernandez, Erosy, and Smith, editors, ANNIE*, 97, 1997.

Multiple targets

- Exclusion radius: ρ_e
- Influence radius: ρ_i
- Measurement subset:
 $R_i \leftarrow R_i^*(r) = \{r_i^j \in R_i : |r_i^j - r| < \rho_i\}$
 $Y_i \leftarrow Y_i^*(r) = \{y(r_i^j) \in Y_i : r_i^j \in R_i^*(r)\}$
- Sliding window:
 $V \leftarrow V^*(r) = \{r^* \in V : |r^* - r| < \max \rho_i\}$

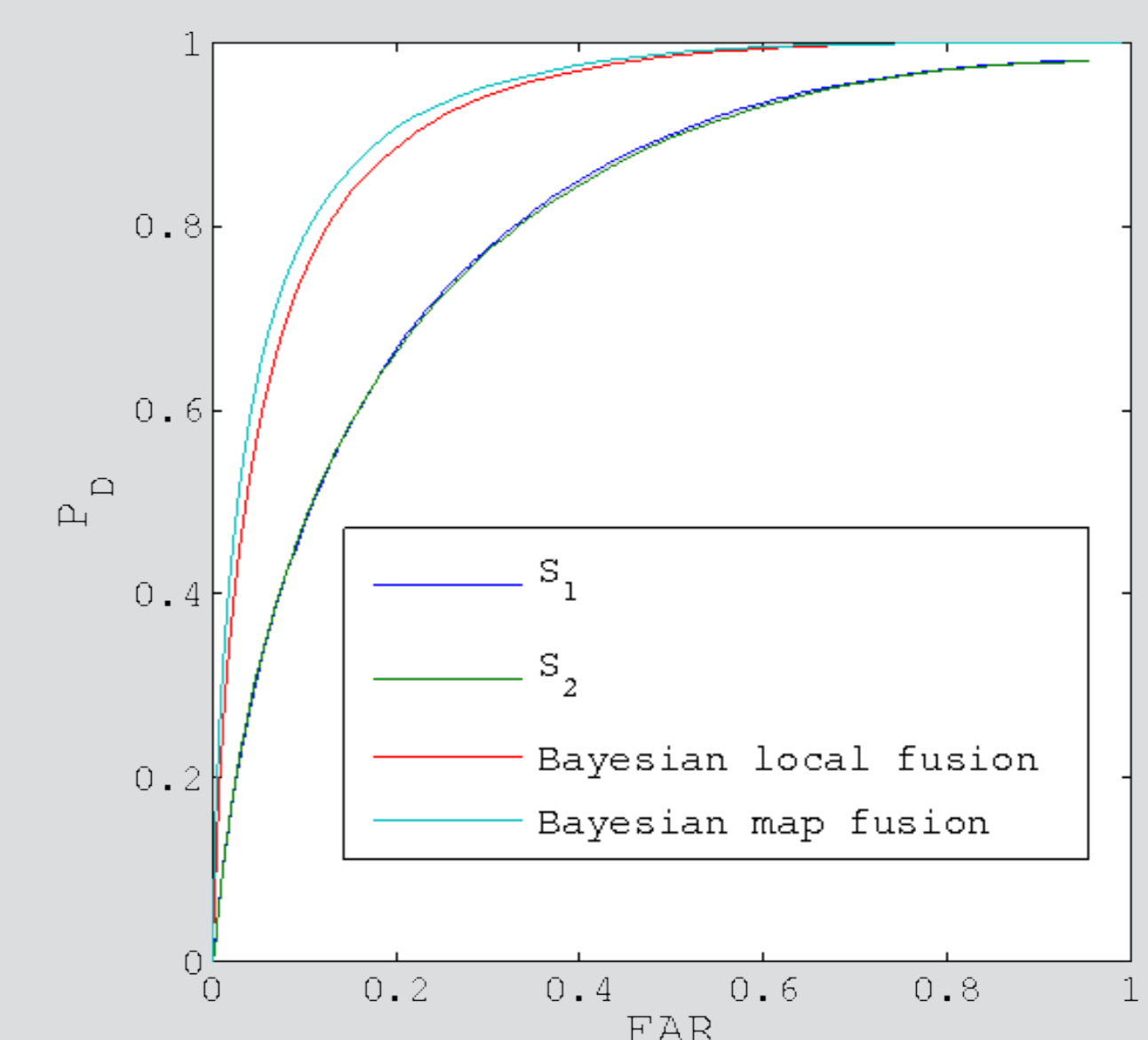


Figure 5: ROC curves for sensors S_1 and S_2 and the output of their Bayesian local fusion [2] and their Bayesian map fusion. ROC curves are obtained by letting vary a threshold on the posterior probabilities $p(T_r|Y_1)$, $p(T_r|Y_2)$ and $p(T_r|Y_1, Y_2)$ on the basis of 10^4 simulations.

Acknowledgment

This work was done at the Royal Military Academy of Brussels for the Belgian Navy Component, in the scope of the study MRN16 funded by the Belgian Ministry of Defense.